

Calcium Imaging of *Drosophila* larvae first order Olfactory Receptor Neurons

Zara Kanold-Tso, Sara Razavi, and Emma Titus
California Institute of Technology

Abstract

In this experiment, we began by using calcium imaging of antennal organs in the brain of *Drosophila melanogaster* larvae to visualize spontaneous neural activity and neural activity in response to odor delivery. More specifically, we used the genetically encoded calcium indicator GCaMP6f and pebbled-Gal4 driver to target olfactory receptor neurons (ORNs). Following issues with image resolution and lack of fluorescence in our larval samples, we pivoted to analyzed calcium imaging fluorescence data from adult *Drosophila* flies in response to wine, apple cider vinegar, ethyl acetate, P-cresol, menthone/methone, and trans-2-hexenal odorants. Results indicated that different regions of interest (ROIs) have distinct inhibitory or excitatory responses. Wine and apple cider vinegar were found to be largely excitatory while menthone and p-cresol were found to be largely inhibitory. Attractive odors were, however, not necessarily excitatory and aversive odors were not necessarily inhibitory, rather each odor is possible a unique combination of excitatory and inhibitory glomeruli.

Introduction

Olfaction is a critical sensory modality for *Drosophila melanogaster*, essential for survival behaviors such as navigation, locating food sources, and avoiding predators and harmful environments throughout both larval and adult stages. This process begins when odorant molecules bind to receptors on olfactory receptor neurons (ORNs), which are housed in peripheral sensory organs. In larvae, ORN axons project directly to the antennal lobe of the central nervous system (CNS), the functional analog of the vertebrate olfactory bulb, where they synapse onto projection neurons within structures called glomeruli (Berck et al.). *Drosophila* larvae possess a relatively simple olfactory system with only 21 ORNs, making them a powerful model for studying the fundamental principles of olfactory coding and behavior (Utashiro et al.).

Drosophila are highly attracted to fermenting and decaying organic matter, such as overripe fruits and vegetables, which release ethyl alcohol, acetic acid, and esters. For the same reason vinegar, wine, and beer, which are all by-products of fermentation, are attractive to the flies. Conversely, they exhibit aversion to certain plant-defense compounds. In this study, we utilized a panel of ecologically relevant odorants: attractive stimuli included wine, apple cider vinegar, ethyl acetate, and p-cresol. Aversive stimuli included methone and trans-2-hexenal. Neutral controls were water and paraffin oil (PFO).

To monitor the activity of these neural circuits, we used calcium imaging, a cornerstone technique in modern neuroscience (Grienberger and Konnerth). Neural firing is tightly coupled

to rapid fluxes in intracellular calcium concentration. By expressing the genetically encoded calcium indicator GCaMP6f in ORNs (using the pebbled-Gal4 driver), we can visualize this activity as changes in fluorescence. This allows for the direct observation of both spontaneous and odor-evoked neural dynamics. We aimed to measure and compare the calcium activity in larval ORNs and their presynaptic terminals in the antennal lobe in response to our odor panel. While our initial larval experiment faced challenges, the analysis of complementary adult *Drosophila* data provided significant insights into the patterns of glomerular activation underlying odor perception.

Results: Larvae Experiment

Despite careful dissection, larval preparations exhibited minimal GCaMP6f fluorescence and poor tissue stability. Rapid degradation of the CNS and motion artifacts precluded reliable quantification of odor-evoked responses. These limitations likely stem from suboptimal mounting, photobleaching, or insufficient expression levels of GCaMP6f in larval ORNs.

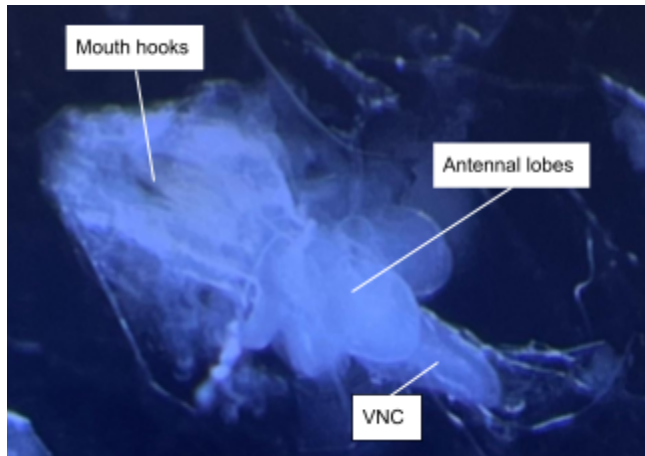


Figure 1. Dissection larval preparation for calcium imaging. Schematic of a pinned *Drosophila* larva expressing GCaMP6f in ORNs, highlighting the mouth hooks, antennal lobes (olfactory center), and ventral nerve cord (VNC). The larva is pinned in saline for live imaging.

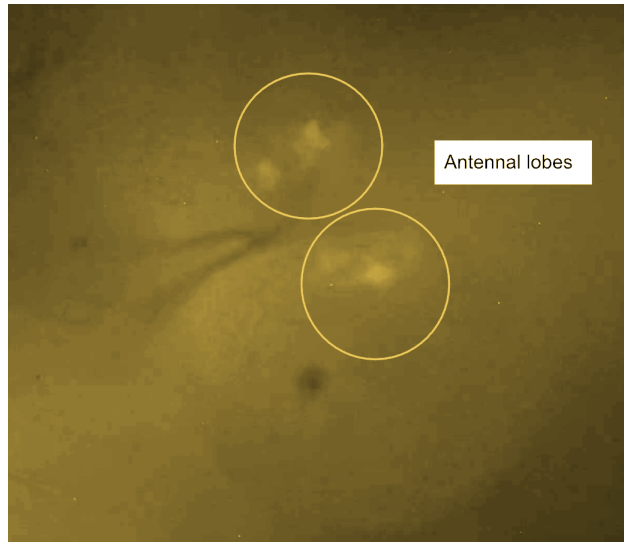
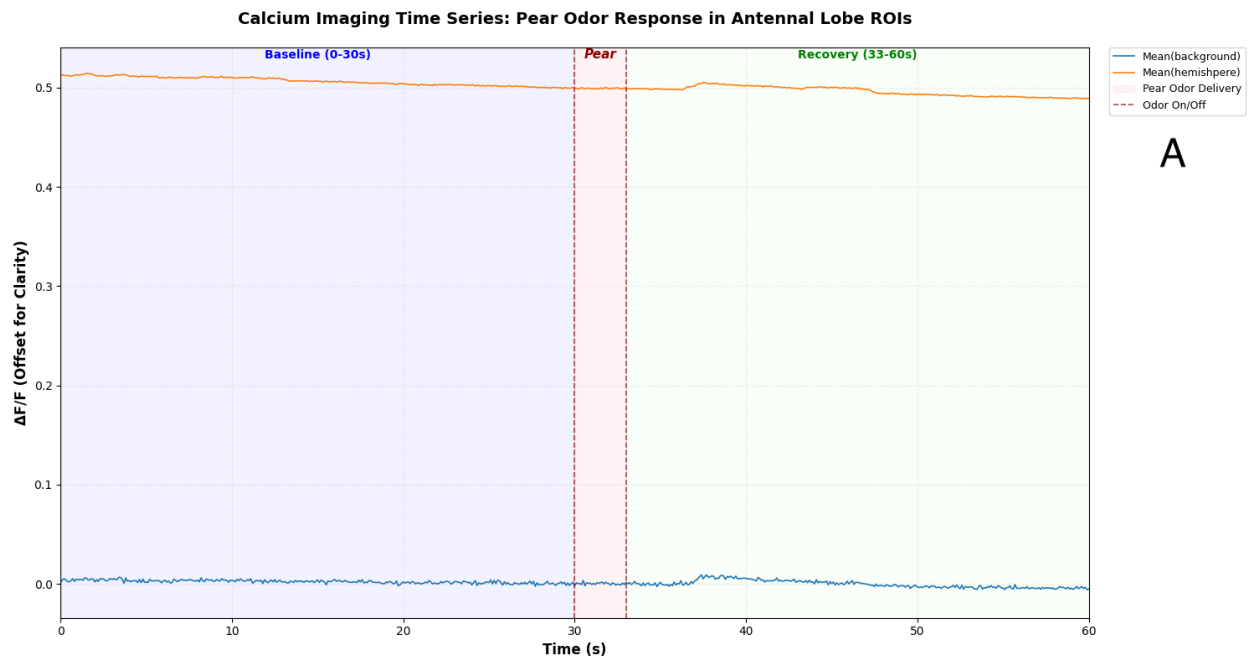


Figure 2. Larval antennal lobe fluorescence. GCaMP6f signal in the larval brain, showing the paired antennal lobes where ORN axons terminate. This baseline image identifies the imaging region for recording calcium activity.



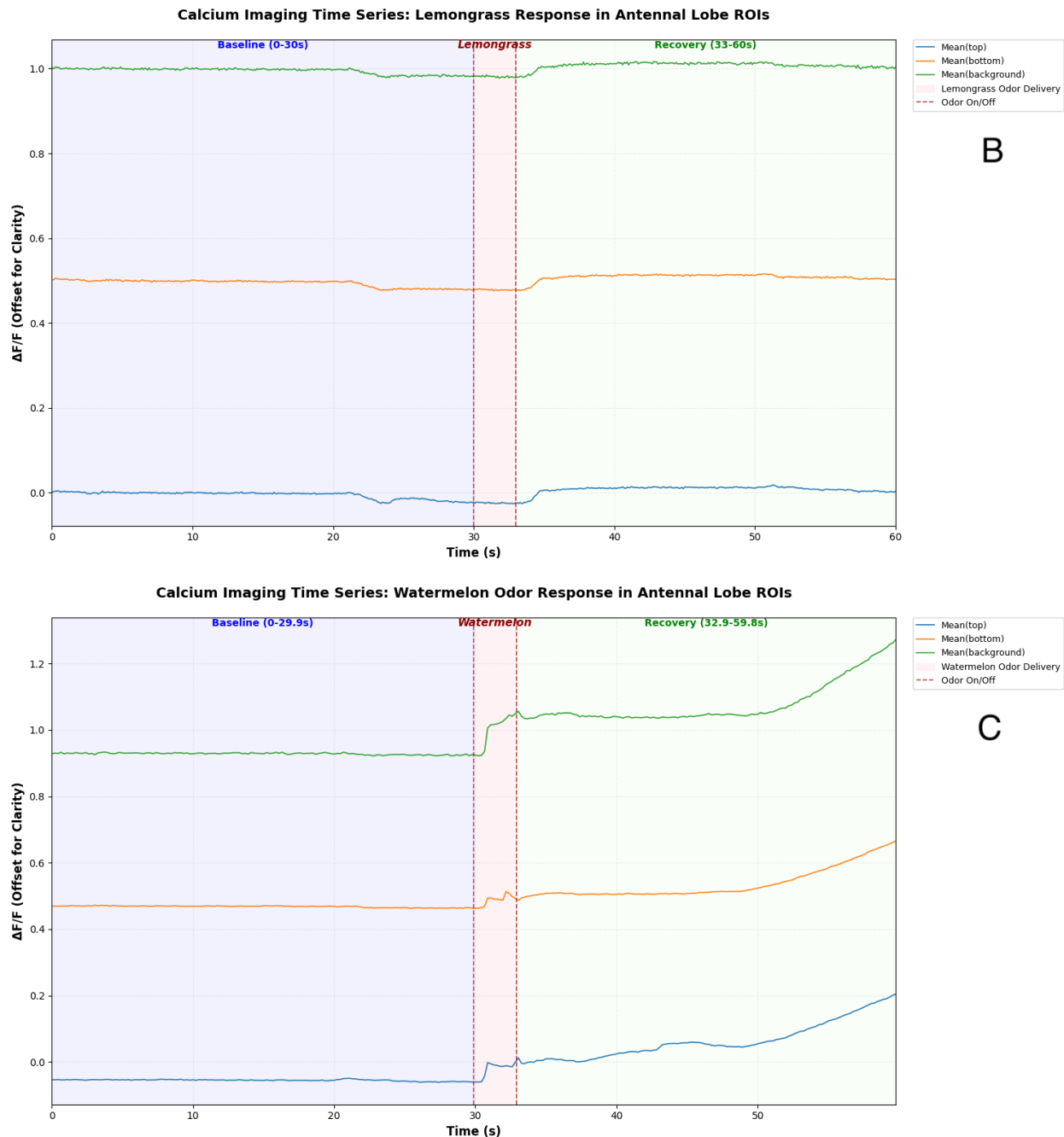


Figure 3. Calcium imaging time series for three attractive odorants delivered to *Drosophila* larvae expressing GCaMP6f in ORNs. Plots show normalized fluorescence ($\Delta F/F$) over time for distinct ROIs within the larva. A) Pear odor evokes no discernable response. B) Lemongrass odor induces a small, transient increase but no clear pattern. C) Watermelon odor shows a gradual, non-specific rise in fluorescence, likely due to motion artifact or background noise rather than a specific neural response. These results highlight the technical limitations encountered in the larval preparation, including low-signal-to-noise ratio and lack of reproducible odor-evoked activity.

Results: Adult *Drosophila* Experiment

Since our original experiment yielded few results, we pivot to analyzing similar data from adult *Drosophila*.

Visual analysis pipeline

To obtain an initial view of the normalized fluorescence before, during, and after odor delivery we can compute the $\Delta F/F$ of a single frame, across all z planes. To do this we first plot a frame during odor delivery (Fig. 4A). Then we calculate the mean fluorescence of the image across the entire time (Fig. 4B). Next, we find the $\Delta F/F$ of the frame by subtracting the mean image from the original frame (Fig. 4C). Finally, we can do this for each z-plane and for the time before, during, and after the stimulus to better compare the response (Fig. 4D).

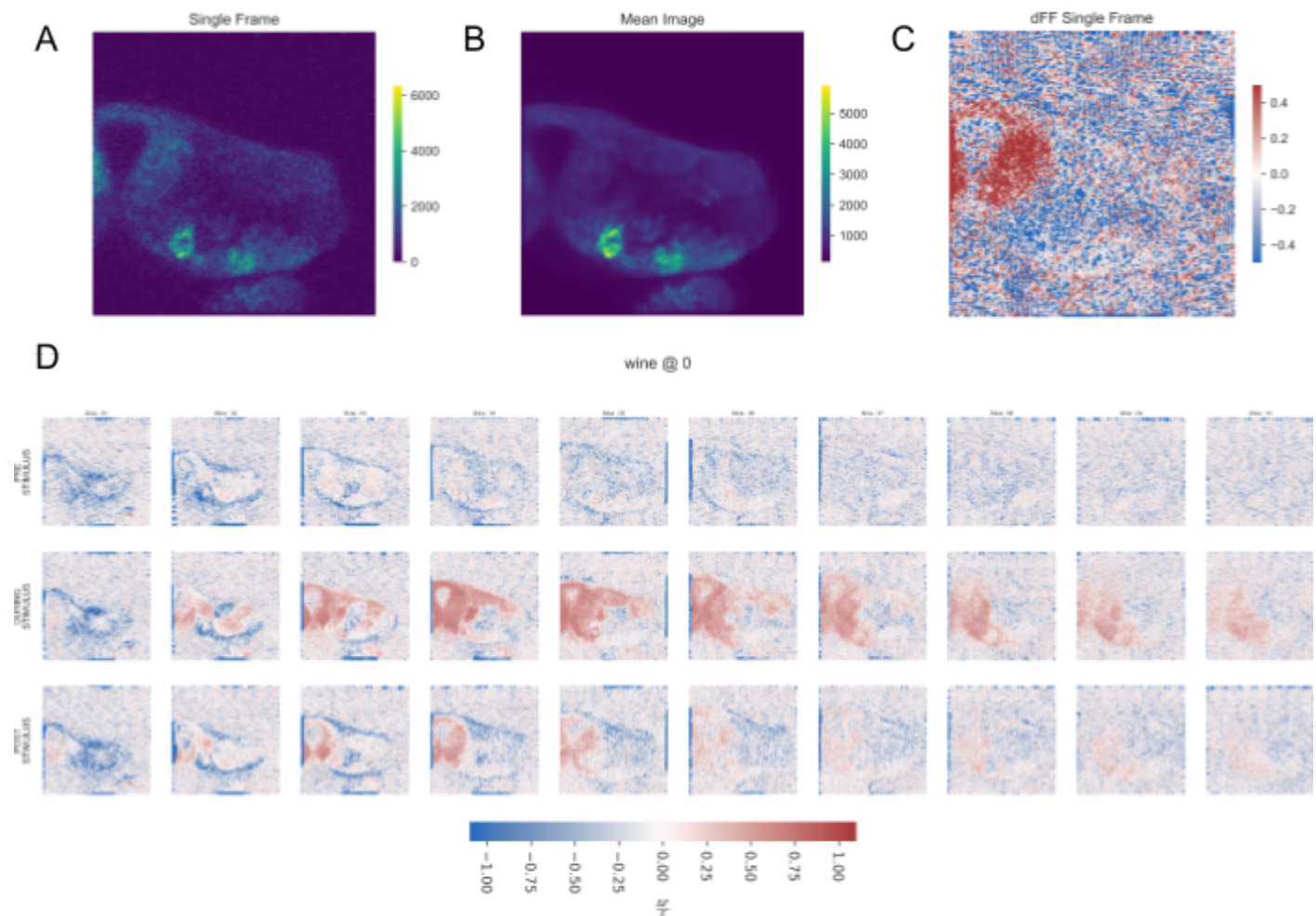


Figure 4. $\Delta F/F$ image creation pipeline. A) Raw fluorescence of a single frame. B) Mean fluorescence across all frames. C) $\Delta F/F$ of a single frame. Created from B-A/B. D) $\Delta F/F$ of adult *Drosophila* antennal lobe before, during, and after the attractive odor wine delivery.

Example of aversive stimulus:

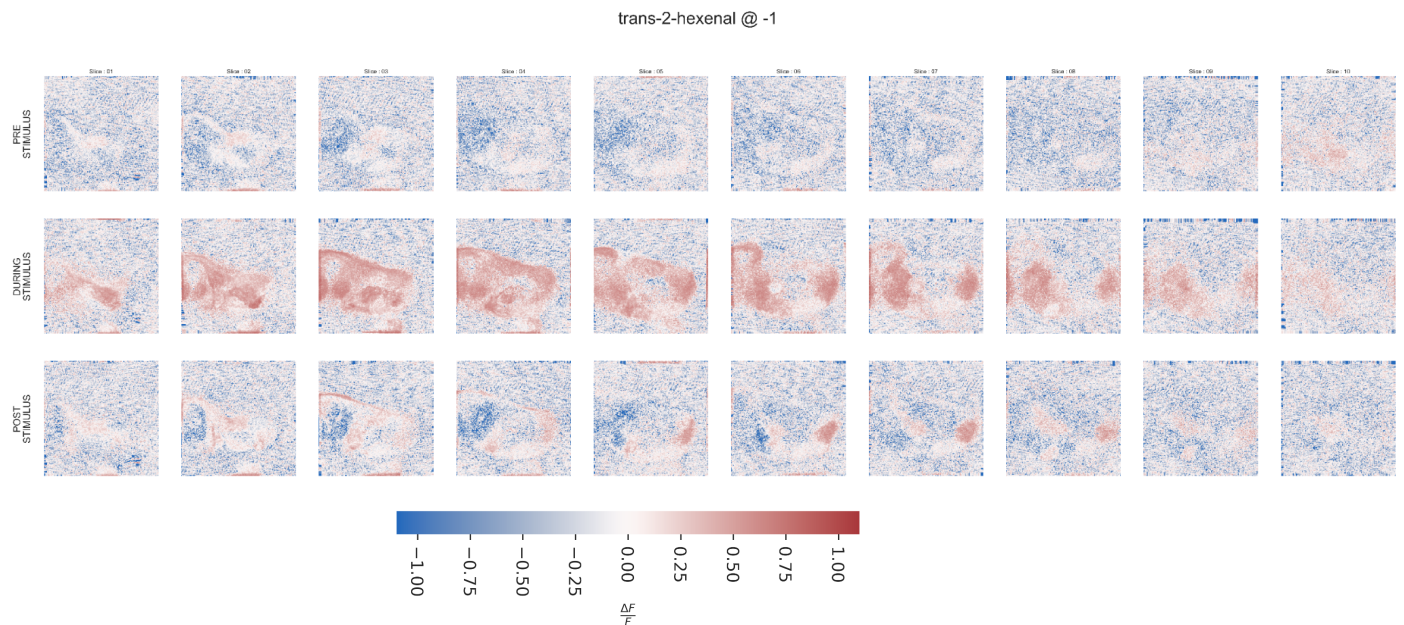


Figure 5. $\Delta F/F$ of adult *Drosophila* antennal lobe before, during, and after the aversive odor trans-2-hexenal delivery.

These graphs are useful for a quick exploratory look at the data but to better quantify the stimuli dependent fluorescence change across smaller areas we analyzed regions of interest (ROIs). The ROIs were roughly determined by eye if they were somewhat independently fluorescing or seem to be a specific region (Fig. 6).

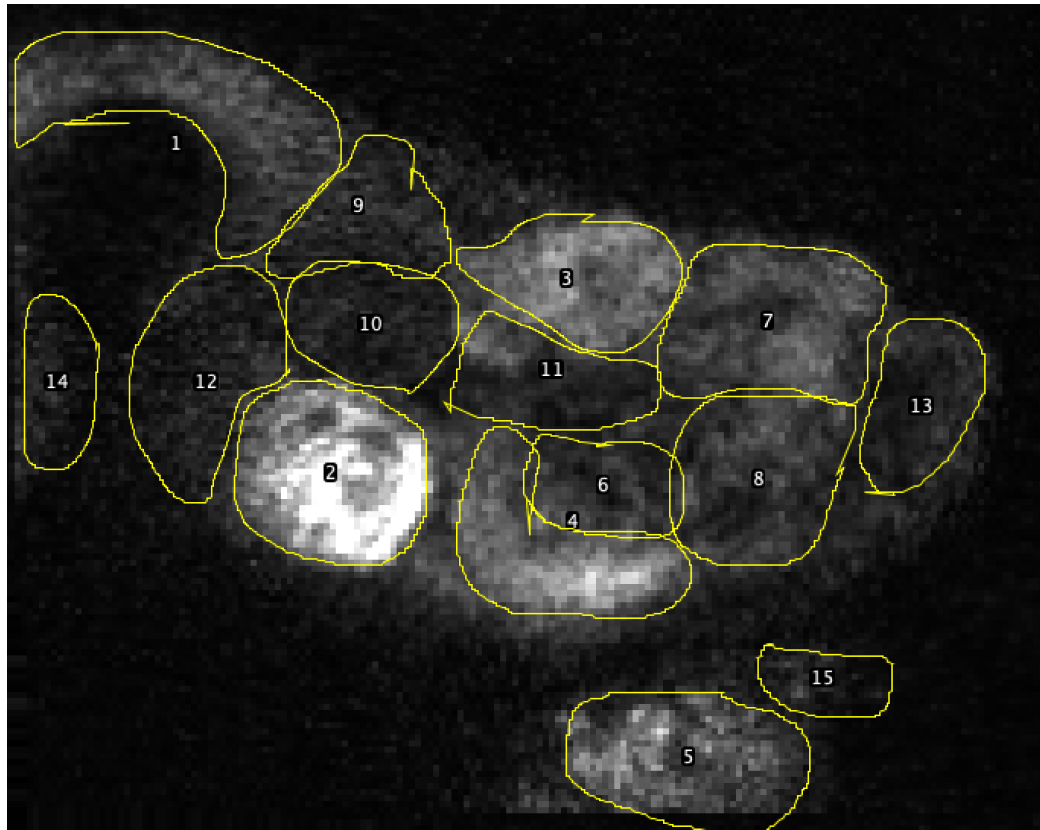


Figure 6. Regions of interest (ROIs) of *Drosophila* antennal lobe. Determined by the eye to look similar to antennal lobe glomeruli or distinct round regions.

We can now plot the time series of fluorescence for each ROI:



Figure 7. Time series plots of each ROIs normalized fluorescence ($\Delta F/F$) with shaded regions indicating which odor is being added. The odors are delivered at different concentrations with @ value * 100 to determine percentage, so @ 0 are pure whereas @ -1 indicated a 10% dilution etc.

Since there are many ROIs and odors, it is difficult to make out many specific conclusions from the time series. However we see distinct peaks and drops for at least a few ROIs during the three trials of each odor delivery.

In order to investigate these changes more specifically, we can create a heatmap of fluorescence change (from baseline) during odor delivery for each ROI and odor.

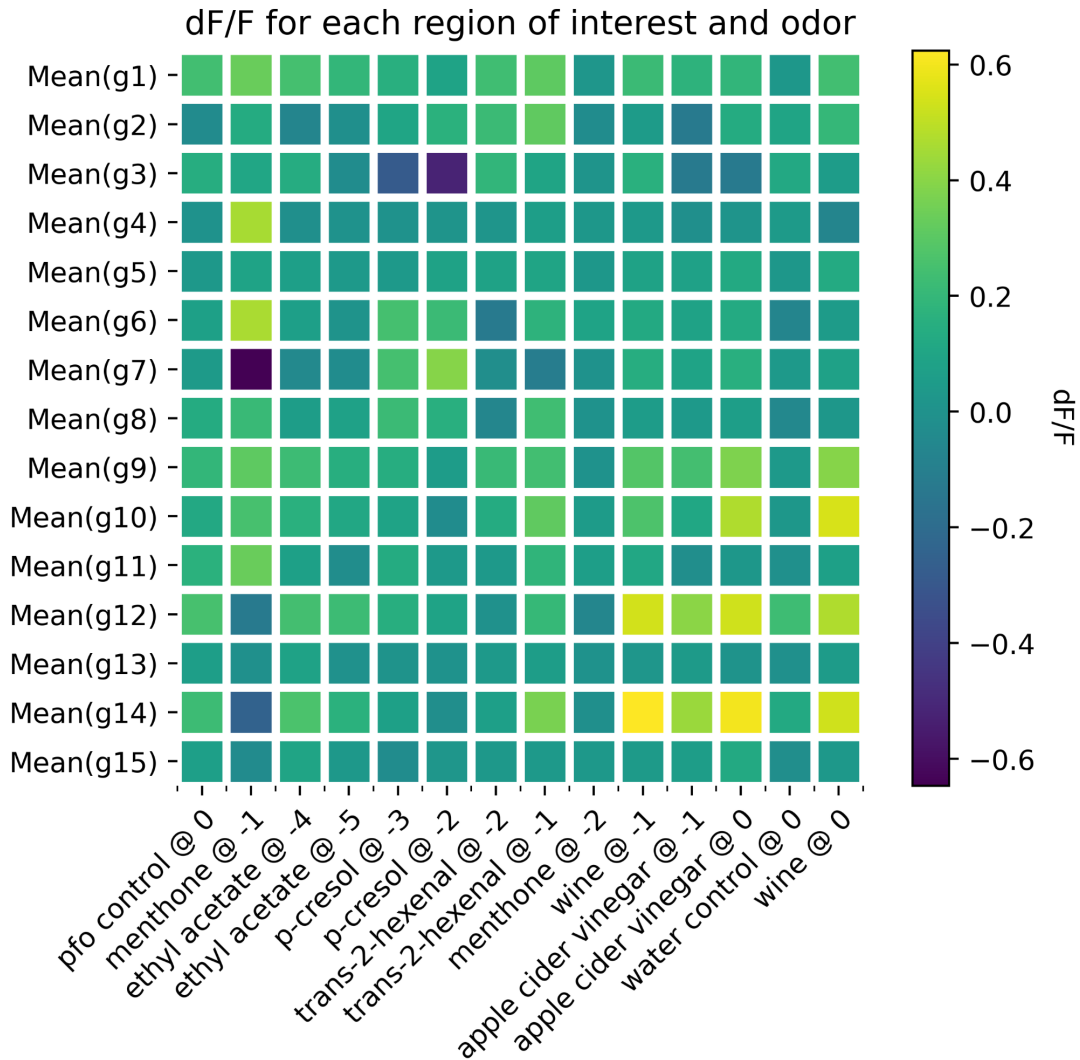


Figure 8. Heatmap of normalized fluorescence change for each ROI during each odor presentation (specifically 2 seconds after initial odor addition).

From the heatmap we can now visually see both excitatory and inhibitory responses to odor stimuli. Wine and Apple cider vinegar show excitatory responses in multiple ROIs. Menthone and p-cresol cause the most prominent inhibitory responses in a few ROIs. However, menthone and p-cresol @ -2 also elicit some excitatory ROIs. The more concentrated trans-2-hexenal shows some excitatory change in a few ROIs, but it is less pronounced than other stimuli, like

wine, at the same concentration. As expected, the controls show little change in fluorescence across ROIs. However, the ROIs during ethyl acetate addition also show little to no changes in fluorescence.

Concentration-Dependent Responses

Because several odorants in the adult dataset were delivered at multiple dilutions, we next examined how glomerular activity scaled with odor concentration. For each odor, we calculated the mean $\Delta F/F$ across all ROIs and plotted these values against odor concentration (Fig. 9).

The resulting concentration-response curves revealed that different odors exhibit distinct tuning patterns rather than a uniform excitatory or inhibitory scaling. Wine shared almost identical responses at 10^{-1} and 10^0 , suggesting that its evoked activity may plateau or saturate at relatively low concentrations. Apple cider vinegar, by contrast, displayed a clear upward trend between 10^{-1} and 10^0 , indicating stronger glomerular response at higher concentrations. Ethyl acetate showed only a small increase between 10^{-5} and 10^{-4} . In contrast to these excitatory patterns, p-cresol responses decreased from 10^{-3} to 10^{-2} , consistent with concentration-dependent inhibition. Menthone showed the opposite pattern, with responses increasing from 10^{-2} to 10^1 , indicating stronger activity, likely inhibitory, in response to higher concentrations.

Trans-2-hexenal exhibited an increase between 10^{-2} to 10^1 , suggesting mild but measurable concentration dependence. Together, these results show that each odorant evokes a unique concentration-dependent response, and that the antennal lobe does not encode odor intensity with a single stereotyped response pattern. Instead, odor identity and concentration are represented through distinct excitatory and inhibitory scaling across ROIs, adding a dynamic dimension to the glomerular code for olfaction.

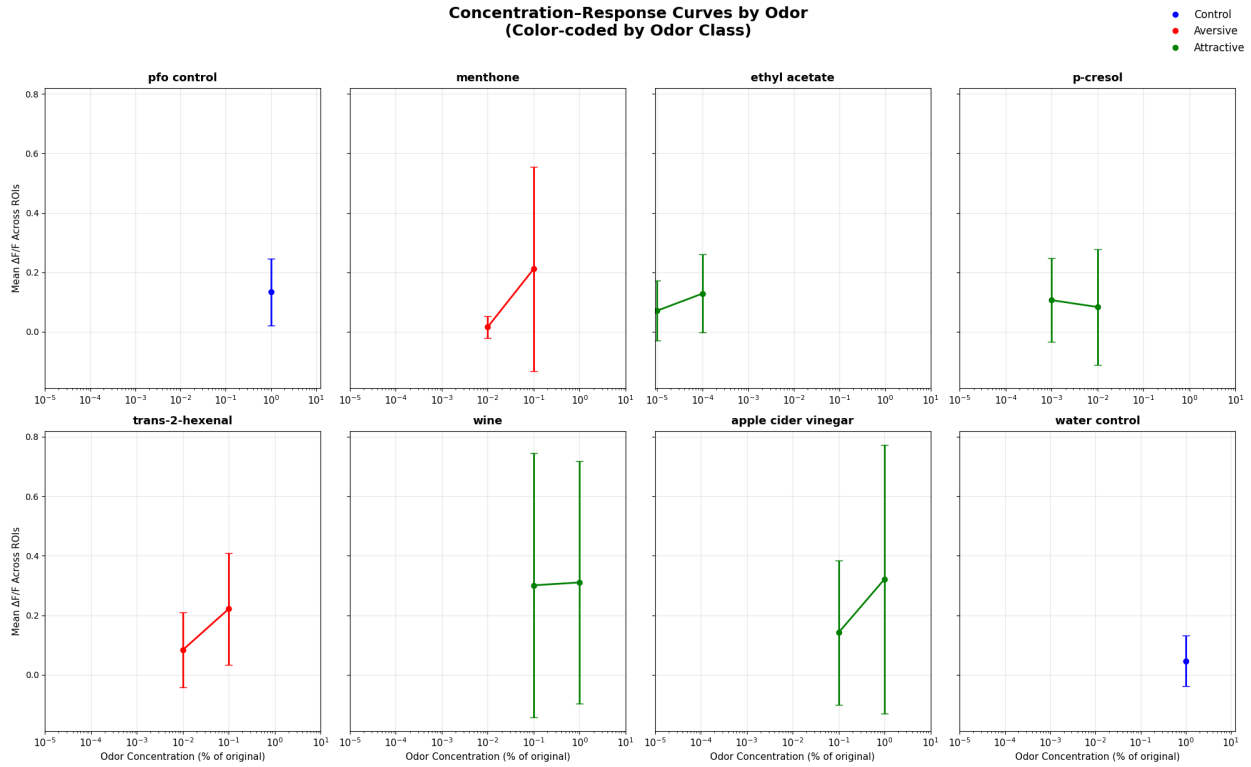


Figure 9. Mean $\Delta F/F$ across all ROIs plotted as a function of odor concentration. Error bars: SD across ROIs. Attractive odors (green), aversive odors (red), controls (blue). Wine shows similar response magnitudes at 10^{-1} and 10^0 , indicating possible saturation at higher concentrations, while apple cider vinegar exhibits a clear concentration-dependent increase. Ethyl acetate shows a small increase from 10^{-5} to 10^{-4} , although overall responses remain weak. p-Cresol displays a decrease in response from 10^{-3} to 10^{-2} , consistent with stronger inhibition at higher concentrations. Menthone and trans-2-hexenal both show increasing responses across concentrations, though with different magnitudes. Water and PFO controls were measured only at one concentration level. These curves highlight the diverse concentration-dependent tuning profiles across odors and demonstrate that odor identity is encoded not only by spatial patterns of ROI activation, but also by how these responses scale with stimulus intensity.

Discussion

Our initial larval experiment was hindered by technical challenges in maintaining viable, intact preparations of the larval CNS with the antennal organ, leading to high variability and insufficient data quality. Future attempts would benefit from optimized dissection protocols, the use of more stable mounting techniques, and potentially the use of a faster imaging system to capture the rapid calcium dynamics in larvae.

After analyzing the adult *Drosophila* data, however, yielded clear and interpretable results. We can see that ROIs have distinct inhibitory and/or excitatory responses. However, attractive odors are not necessarily excitatory and aversive odors are not necessarily inhibitory. Rather each odor may be encoded by a unique combination of excitatory aversive responses. Our ROIs may

include some distinct glomeruli since they're somewhat easy to distinguish visually. Therefore, the different glomeruli responses may encode olfactory data. However, further work, where the glomeruli are distinguished, is needed to test these claims.

Overall, this study demonstrates the power of calcium imaging to resolve the functional organization of the olfactory system. It confirms that even at the first synaptic level in the brain, odor identity is represented by a complex glomerular map. Future work should focus on correlating these calcium activity patterns with specific, identifiable glomeruli and link them directly to behavioral outputs to build a complete understanding of olfactory-driven behavior.

Methods: Larvae Experiment

Sample preparation

Acquired pebbled-Gal4 x UAS-GCaMP6f *Drosophila* larvae from the Hong lab. The dissected larvae: retaining brain, VNC, and antennal organ was pinned to a dish containing saline.

Odorant delivery

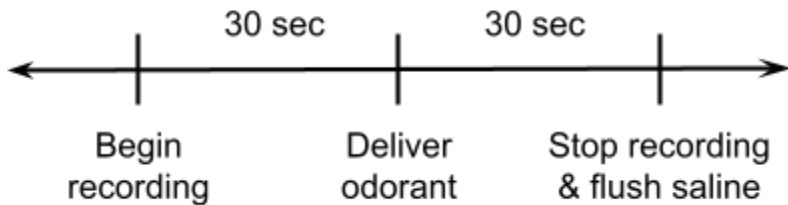


Figure 10. Experimental Protocol. Thirty seconds of spontaneous activity before and after odor delivery were recorded.

Odors, acquired from the Hong lab, were suspended in either water or paraffin oil. Attractive odors: pear, watermelon, and banana were added to the dish's saline via syringe. Aversive odors: peppermint, lemongrass, and 3-octanol were also tested. Saline alone was also added as a control for possible odor delivery noise.

After recording, odors were flushed from the dish using two syringes: one adding and one removing ~10 ml net saline total.

Imaging Settings

Imaged using a 12x lens submerged in saline. 4x4 binning was used to reduce file size since we had an acquisition frame rate of 10 Hz. We used an exposure time of ~100 ms with ~20 dB gain.

Methods: Adult *Drosophila* Experiment

Sample preparation

Adult *Drosophila*, from the Hong lab, were dissected to expose antennal lobes and glue humerus to sample holder slightly upward angled to promote walking.

Odorant delivery

Constant flowing saline wherein odors are delivered three times (with 20s interval) then flushed. Odors were suspended in either water or paraffin oil. Attractive odors: apple cider vinegar, wine, p-cresol, and ethyl acetate were tested. Aversive odors: menthone and trans-2-hexenal were also tested. Pure water and paraffin oil (PFO) were also added as controls.

Imaging Settings

2-photon imaging of GCamp6f was performed at 0.5 Hz.

Analysis

Videos were opened in ImageJ/FIJI and data from circled ROIs exported for statistical analysis. Adult *Drosophila* data was acquired from Pratyush Kandimalla (Hong lab) and analyzed in Jupyter Lab using custom python scripts and python scripts from Kandimalla.

References

Matthew E Berck, Avinash Khandelwal, Lindsey Claus, Luis Hernandez-Nunez, Guangwei Si, Christopher J Tabone, Feng Li, James W Truman, Rick D Fetter, Matthieu Louis, Aravinthan DT Samuel, Albert Cardona (2016) The wiring diagram of a glomerular olfactory system eLife 5:e14859.

Grienberger C, Konnerth A. Imaging calcium in neurons. *Neuron*. 2012 Mar 8;73(5):862-85. doi: 10.1016/j.neuron.2012.02.011. PMID: 22405199.

Utashiro, N., Williams, C.R., Parrish, J.Z. et al. Prior activity of olfactory receptor neurons is required for proper sensory processing and behavior in *Drosophila* larvae. *Sci Rep* 8, 8580 (2018). <https://doi.org/10.1038/s41598-018-26825-3>

Supplementary Material

Since this paper cannot fit the large DF/F images with good resolution we encourage you to consult the supplement below for the DF/Fs for each stimuli.

 [Drosophila_odor_presentation](#)

https://docs.google.com/presentation/d/1ip6Eaz5qdZX5biI2aWtR6HBG0XcpBoXOQb_NEvCSVig/edit?usp=sharing